Molecular Genetics and Metabolism Reports 21 (2019) 100525

Contents lists available at ScienceDirect

Molecular Genetics and Metabolism Reports

journal homepage: www.elsevier.com/locate/ymgmr

Identification of mutations in Malaysian patients with argininosuccinate lyase (ASL) deficiency

Ernie Zuraida Ali[a,*], Yusnita Yakob[b], Lock Hock Ngu[c,*]

[a] Inborn Error of Metabolism and Genetic Unit, Nutrition, Metabolism and Cardiovascular Research Centre, Institute for Medical Research, National Institutes of Health, Ministry of Health Malaysia, Section U13 Setia Alam, 40170 Shah Alam, Selangor, Malaysia

[b] Molecular Diagnostics and Protein Unit, Specialized Diagnostics Centre, Institute for Medical Research, National Institutes of Health, Ministry of Health Malaysia, Jalan Pahang, 50588 Kuala Lumpur, Malaysia

[c] Medical Genetics Department, Kuala Lumpur Hospital, Ministry of Health Malaysia, Jalan Pahang, 50588 Kuala Lumpur, Malaysia

ARTICLE INFO

Keywords:
Argininosucinate lyase deficiency
ASLD
Autosomal recessive
Mutation
Hyperammonemia

ABSTRACT

Argininosuccinate lyase (ASL) deficiency impairs the function of the urea cycle that detoxifies blood ammonia in the body. Mutation that occurs in the *ASL* gene is the cause of occurrence of ASL deficiency (ASLD). This deficiency causes hyperammonemia, hepatopathy and neurodevelopmental delay in patients. In this study, the clinical characteristics and molecular analysis of 10 ASLD patients were presented. 8 patients were associated with severe neonatal onset, while the other 2 were associated with late onset. Molecular analysis of *ASL* gene identified four new missense variants, which were c.778C > T, p.(Leu260Arg), c.1340G > C, p.(Ser447Thr), c.436C > G, p.(Arg146Gly) and c.595C > G, p.(Leu199Val) and four reported missense variants, which were c.638G > A, p.(Arg213Gln); c.556C > T, p.(Arg186Trp), c.578G > A, p.(Arg193Gln) and c.436C > G, p.(Arg146Trp). *In silico* servers predicted all new and reported variants as disease-causing. Structural examination exhibited that all pathogenic variants affected the stability of the tetrameric ASL structure by disturbing the bonding pattern with the neighboring residues.

Conclusion: This study revealed the genetic heterogeneity among Malaysian ASL patients. This study has also expanded the mutational spectrum of the ASL.

1. Introduction

Argininosuccinate lyase deficiency (ASLD) is an autosomal recessive urea cycle disorder causing argininosuccinic aciduria. Argininosuccinate lyase (ASL; MIM 608310) is one of the six enzymes in urea cycle that converts waste nitrogen into urea. ASL involves in the fourth step of the urea cycle by catalyzing argininosuccinic acid (ASA) to produce arginine and fumarate [1,2]. Mutations in the *ASL* gene result in defective cleavage of ASA leading to an accumulation of ASA in cells and an excessive excretion of ASA in urine. ASLD can manifest a wide clinical spectrum from asymptomatic to severe hyperammonemic neonatal onset life-threatening courses. The estimated incidence of ASLD is approximately one in 218,750 live births making it the second most common disorder in the urea cycle [3]. The diagnosis of ASLD is established based on elevation of plasma citrulline together with elevated argininosuccinic acid in the plasma or urine and can be confirmed by assay of ASL enzyme activity or molecular genetic testing of *ASL* gene, the latter of which offers additional advantages for genetic counselling of the family or prenatal testing in later pregnancies [4].

The human *ASL* gene is located on chromosome 7q11.21 [5], spans approximately 17 kb and comprises of 16 coding exons encoding 464 amino acids. ASL is a homotetramer of ~52kDA subunit and is considered as the mature enzyme carrying four identical active sites which provide binding pockets for ASA [6]. The enzyme is located in the cytosol and is expressed predominantly in liver [1]. However, it is also detected in many other tissues, including kidney [7], small intestine [8] and brain [9].

To date, there are 167 variants of the *ASL* gene reported by the Human Gene Mutation Database (HGMD) (http://www.hgmd.cf.ac.uk) [10], a database that provides information on DNA variants with current listing of 107 variants in its public site and 160 variants in the professional version 2018. Majority of variants are missense, but almost all types of other variants are also found. Even though > 160 ASL variants have been described, however the genotype-phenotype correlations are still not completely clear as standard biochemical testing is not sensitive enough to measure residual activity. Other possible factors

* Corresponding authors.
E-mail addresses: ernie@imr.gov.my (E.Z. Ali), ngu.lockhock@moh.gov.my (L.H. Ngu).

https://doi.org/10.1016/j.ymgmr.2019.100525
Received 29 July 2019; Received in revised form 16 September 2019; Accepted 16 September 2019
Available online 24 October 2019

such as ASL tissue-specific expression [11], methylation status [12] and frequent alternative splicing variants [13] may influence the clinical phenotype. In this study, we present the molecular characterization of 10 patients affected with ASLD by analyzing the *ASL* gene and structure.

2. Materials and methods

2.1. Patients

This study includes samples from 10 patients from a total of 10 different families diagnosed with ASLD at Kuala Lumpur Hospital (HKL). All patients were identified to have ASLD according to clinical observations and metabolic findings. To confirm the diagnosis, molecular genetic testing was carried out to all patient samples, at Molecular Diagnostics and Protein Unit (UMDP), Institute for Medical Research. Once mutation was identified in the patients, clinicians would call parents to test the inheritance cases. Only parent samples from 5 patients were available and all parents were healthy. The control group was also included in this study which consisted of 50 normal healthy individuals. Informed consent was obtained from all patients. Peripheral blood (approximately 5 to 10 mL) was collected inside a standard EDTA tube. This study was performed according to the Declaration of Helsinki.

2.2. DNA extraction, PCR and sequencing

The genomic DNA from all blood samples were extracted by using the DNA Blood Mini Kit (QIAGEN, Hilden, Germany). The *ASL* gene including intron-exon boundaries [14] was amplified using the touchdown polymerase chain reaction (PCR) method. The amplified PCR product was run on 1.5% agarose gel under standard electrophoresis.

The PCR product was purified by using the QIAquick PCR purification kit (QIAGEN, Hilden, Germany) and cycle sequencing was then carried out by using the Big Dye Terminator cycle sequencing version 3.1 (Applied Biosystems, Foster City, CA). The sequencing reaction was then electrophoresed by the Applied Biosystems 3500 Genetic Analyzer.

2.3. Mutation confirmation

SeqScape Software version 2.5 (Applied Biosystems, Foster City, CA) was used to identify the DNA variants, in which the sequencing results were aligned to the genomic and coding DNA reference sequence of *ASL* gene (NC_000007.13 and NM_000048.3). Human genome GRCh37/hg19 was used to retrieve all reference sequences. The single nucleotide variants (SNVs), insertion and deletion were reported by referring to the Human Genome Variation Society (HGVS) (http://www.hgvs.org/mutnomen).

Identified variants were compared against two public databases; HGMD [10] and 1000 Genome Project data (http://www.1000genomes.org) [15] in order to differentiate the one as reported or new variants. Meanwhile, the new variants were then compared with 50 healthy normal individuals (100 alleles) and Genome Aggregation Database (gnomAD) [16] in order to rule out a polymorphism.

2.4. In silico prediction

To validate the degree of conservation, HomoloGene program (http://www.ncbi.nlm.nih.gov/homologene) was used to run the multiple-sequence alignment. Meanwhile, the pathogenicity of missense variants was then predicted using four *in silico* webservers, FATHMM-XF [17], Mutation Taster2 [18], M-CAP [19] and PROTEAN [20]. Missense variants predicted as damaging by at least three or more servers were considered as disease-causing. In addition, I-Mutant 3.0 server [21], CUPSAT [22] and Site Directed Mutator (SDM) [23] were used to predict the stability/instability of the protein. Missense variants were considered as destabilizing in nature if two or more than two algorithms showed a decrease in stability upon mutation.

2.5. Modeling of native and mutant ASL structures

The effects of missense variants on the protein structure were then observed through computational modeling. The human ASL X-ray crystal structures were retrieved from the Protein Databank (RCSB-PDB) [24]. At the moment, two human ASL X-ray crystal structures were crystallized with resolutions 4.2 Å (PDB ID: 1AOS) [25] and 2.65 Å (PDB ID: 1K62) [26]. However, structure with resolution 4.2 Å consisted missing residues, while structure with resolution 2.65 Å had a mutation at residue 286. Therefore, the three dimensional (3D) ASL native model was built using SWISS-MODEL program [27] by submitting the targeted sequence (native) to the program. The ASL mutant model was generated *via* the Swiss-PDB viewer [28]. The 'Mutate' tool in the Swiss-PDB viewer was used to change the target amino acid in the ASL native model. Once the ASL native and mutant models were generated, energy minimizations were then performed using the same program to remove unwanted contacts. The GROMOS96 force field was used to assign the atomic charges to all the residues. The ASL native and mutant models were then visualized using PyMol software [29].

2.5.1. Native and mutant models validation

The qualities of the ASL native and mutant models were validated using ProCheck [30], ProSA-web [31] and ERRAT [32] programs. The Ramachandran plot generated by the ProCheck program was used to verify the overall stereochemical quality and accuracy of the predicted model. The geometry of the residues from the predicted model was compared with the X-ray crystal or NMR structures. The good quality of predicted model which covers the residues located in the most favorable and additional allowed region should be > 90%.

The ProSA-web used molecular mechanics force field [31] to calculate energy profiles (z-score) for the modeled structures. The z-score predicts overall model quality and measures the total energy deviation of the structure using random conformations. The modeled structure is predicted to be erroneous if the z-scores range beyond the characteristic of reference proteins. Meanwhile, for better interpretation of the predicted protein, the z-score plot can be used to check whether the z-score of the predicted protein is within the range of scores typically found for proteins of similar groups.

ERRAT was used to inspect the correctness of the overall fold/structure and faults over localized regions. ERRAT score provides the whole quality factor for non-bonded atomic interactions. Score > 50% indicates the higher quality model. The quality of the ASL native and mutant models were also verified by calculating the root mean square deviation (RMSD) using the Swiss-PDB viewer. The RMSD of the native model was calculated by superimposing the native model with the template structure (PDB ID: 1K62). Meanwhile for the mutant models, the RMSDs were calculated by superimposing the mutant models with the native model.

2.5.2. Hydrogen bond analysis

The hydrogen bond interaction between native and neighboring residues was analyzed using Chimera software [33]. The relax hydrogen bond constraint was set to be within 0.4 Å with a maximum angle of 30 degree.

3. Results

3.1. Clinical findings

Ten patients (4 males and 6 females) from ten families were studied. All patients except one (Patient P7) were from Malay ethnicity background. Table 1 presents the main clinical features of these patients. Eight patients have had their first presentation during neonatal period,

Table 1
Summary of clinical and biochemical features of argininosuccinate lyase deficiency (ASLD) patients.

Patient	Sex	Initial presentation					Subsequent clinical progress	Family history
		Age	Presenting symptoms	Blood ammonia, μmol/L, N.R. < 51)	Therapy received	Outcome		
P1	F	25d	Poor suck, lethargy, myoclonus seizures, acute change in sensorium	264	SPI, PFN, SB, SPB, L-Arg	Survived	Spastic tetraplegia, severe psychomotor retardation, frequent seizure episodes despite a low-protein diet and treatment with oral ammonia scavengers, fatal encephalopathy at 21 y	CP, one affected elder sibling
P2	F	10d	Recurrent vomiting, difficulty in breathing, acute encephalopathy	210	SPI, PFN, SB, SPB, L-Arg	Survived	MLD, infrequent decompensation on a low-protein diet and oral ammonia scavengers. Current age is 13y.	NCP, no other affected family member
P3	F	5d	Vomiting, lethargy, breathing abnormalities	274	Protein restriction, SB, L-Arg	Survived	MLD, no acute decompensation on a low-protein diet and oral ammonia scavengers. Current age is 24y.	NCP, one affected elder sibling died at 9y (undiagnosed)
P4	M	5d	Feeding intolerance, irritability, altered sensorium	501	SPI, PFN, SB, SPB, L-Arg, DL, MV	Survived	MDD/LD, recurrent decompensation during first 2 years. Current age is 8y	NCP, no other affected family member
P5	M	4d	Feeding intolerance, irritability, progressing to somnolence	446	SPI, PFN, SB, SPB, L-Arg, MV	Survived	MLD, infrequent decompensation on a low-protein diet and oral ammonia scavengers. Current age is 11y. -	NCP, one affected elder sibling died at 3 m
P6	M	5d	Feeding refusal, vomiting, lethargy, breathing abnormalities, progressing to coma	510	SPI, PFN, SB, SPB, L-Arg, DL, MV	Survived	SLD, recurrent decompensation during first 5 years. Current age is 14y	NCP, no other affected family member
P7	M	5y	Drowsy, seizures, feeding refusal preceded by a febrile illness	ND	SPI, PFN	Survived	MLD, no further decompensation on a low-protein diet. Current age is 11y.	NCP, no other affected family member
P8	F	3d	Abnormal breathing, progressive acute encephalopathy	305	SPI, PFN, SB, SPB, L-Arg, MV	Survived	MLD, infrequent decompensation on a low-protein diet and oral ammonia scavengers. Current age is 12y.	NCP, no other affected family member
P9	F	7d	Vomiting, lethargy, seizures, progressing to coma	447	SPI, PFN, SB, SPB, L-Arg, MV	Survived	SDD, recurrent decompensation on a low-protein diet and oral ammonia scavengers. Died at 6y.	NCP, no other affected family member
P10	F	6y	Learning disabilities, hyperactivity	78	Protein restriction, SB, L-Arg	Survived	MLD, no acute decompensation on a low-protein diet and oral ammonia scavengers. Current age is 12y.	NCP, no other affected family member

M male, *F* female, *y* years, *m* month, *d* days, *SPI* Stop protein intake, *PFN* Parenteral fluid and nutrition, *L-Arg* L-arginine, *SB* sodium benzoate, *SPB* sodium phenylbutyrate, *DL* dialysis, *MV* Mechanical ventilation, *MLD* Mild learning disability, *MDD/LD* Moderate developmental delay/learning disability, *SLD* Severe learning disability, *SDD*. Severe developmental delay, *ND* not done, *CP* Consanguineous parents, *NCP* Non-consanguineous parents.

Table 2
Mutations identified, *in-silico* servers prediction and population frequency of the alleles in ASLD patients.

Patient	Mutation state	Exon/ intron	Mutation			Type of mutation	Gene conservation in eukaryota (%)	Deleterious or damaging prediction		
			Genome number (GRCh37/hg19)	Coding DNA number	Protein number			FATHMM-XF	Mutation taster2	M-CAP
P1	HM	Ex-8	g.65552356G > A	c.638G > A	p.(Arg213Gln)	M	100	D	DC	PP
P2	HM	Ex-8	g.65552356G > A	c.638G > A	p.(Arg213Gln)	M	100	D	DC	PP
P3	HM	Ex-8	g.65552356G > A	c.638G > A	p.(Arg213Gln)	M	100	D	DC	PP
P4	HT	Ex-8	g.65552356G > A	c.638G > A	p.(Arg213Gln)	M	100	D	DC	PP
P5	HM	Ex-7	g.65551762C > T	c.556C > T	p.(Arg186Trp)	M	100	D	DC	PP
P6	HM	Ex-7	g.65551762C > T	c.556C > T	p.(Arg186Trp)	M	100	D	DC	PP
P7	CHT	Ex-7	g.65551784G > A	c.578G > A	p.(Arg193Gln)	M	100	D	DC	PP
		Ex-10	g.65553853C > T	c.778C > T	p.(Leu260Phe)	M	100	D	DC	PP
P8	CHT	Ex-5	g.65548151C > T	c.436C > T	p.(Arg146Trp)	M	90	D	DC	PP
		Ex-15	g.65557844G > C	c.1340G > C	p.(Ser447Thr)	M	90	D	DC	PP
P9	HM	Ex-5	g.65548151C > G	c.436C > G	p.(Arg146Gly)	M	90	D	DC	PP
P10	CHT	Ex-7	g.65551762C > T	c.556C > T	p.(Arg186Trp)	M	100	D	DC	PP
		Ex-7	g.65551801C > G	c.595C > G	p.(Leu199Val)	M	100	D	DC	PP

Patient	Deleterious or damaging prediction		Stability prediction				Screening with 100 normal alleles	Population allele frequency from gnomAD database	Reference
	PROTEAN	Consensus	I-mutant 3.0	CUPSAT	SDM	Consensus			
P1	Del	4/4	I	DS	RS	2/3	–	–	(34)
P2	Del	4/4	I	DS	RS	2/3	–	–	(34)
P3	Del	4/4	I	DS	RS	2/3	–	–	(34)
P4	Del	4/4	I	DS	RS	2/3	–	–	(34)
P5	Del	4/4	D	DS	RS	3/3	–	–	(36)
P6	Del	4/4	D	DS	RS	3/3	–	–	(36)
P7	Del	4/4	D	DS	RS	3/3	–	–	(37)
	Del	4/4	D	DS	RS	3/3	A	A	This study
P8	Del	4/4	D	DS	IS	3/3	–	–	(34)
	Del	4/4	D	S	RS	2/3	A	A	This study
P9	Del	4/4	D	DS	RS	3/3	A	A	This study
P10	Del	4/4	D	DS	RS	3/3	–	–	(36)
	Del	4/4	D	DS	RS	3/3	A	A	This study

HM homozygous, *HT* heterozygous, *CHT* compound heterozygous, *M* missense, – not calculable, *D* damaging, *DC* disease causing, *PP* possibly pathogenic, *Del* deleterious, *Inc* increase, *Dec* decrease, *DS* destabilizing, *S* stabilizing, *RS* reduce stabilizing, *IS* increase stabilizing, *A* absence, *P* presence.

Table 3
Evaluation of ASL native and mutant models by using PROCHECK, ProSA-Web and ERRAT programs.

Patient	Exon	Mutation		Ramachandran plot statistics (%)				ProSA	Errat (%)	RMSD (Å)
		Coding DNA number	Protein number	Most favoured	Additionally allowed	Generously allowed	Disallowed	z-Score	Overall quality factor Score	
Native				94.4	5.1	0.5	0.0	−8.61	95.37	0.05
P1	Ex-8	c.638G > A	p.(Arg213Gln)	94.4	5.1	0.5	0.0	−8.59	95.83	0.01
P2										
P3										
P4										
P5	Ex-7	c.556C > T	p.(Arg186Trp)	94.2	5.3	0.5	0.0	−8.58	93.06	0.05
P6										
P7	Ex-7	c.578G > A	p.(Arg193Gln)	94.4	5.1	0.5	0.0	−8.59	95.37	0.01
	Ex-10	c.778C > T	p.(Leu260Phe)							
P8	Ex-5	c.436C > T	p.(Arg146Trp)	94.2	5.3	0.5	0.0	−8.66	93.52	0.05
	Ex-15	c.1340G > C	p.(Ser447Thr)							
P9	Ex-5	c.436C > G	p.(Arg146Gly)	94.2	5.3	0.5	0.0	−8.63	93.06	0.05
P10	Ex-7	c.556C > T	p.(Arg186Trp)	94.2	5.3	0.5	0.0	−8.66	93.06	0.05
	Ex-7	c.595C > G	p.(Leu199Val)							

with blood ammonia ranging from 210 μmol/L to 510 μmol/L and required emergency treatment. Two patients, P7 and P10 presented at later age, at 5 years and 6 years old respectively. Despite dietary protein restriction and ammonia scavengers therapy, all patients had impaired cognitive function: 6 with mild learning disabilities, 1 with moderate learning disabilities, and 3 with severe learning disabilities.

3.2. Molecular diagnosis

Table 2 shows direct sequencing result of *ASL* gene in the ten patients. Six (60%) patients were in homozygous state, three (30%) patients were in compound heterozygous state and one (10%) patient was in heterozygous state (Table 2). Eight missense variants (c.638G > A; c.556C > T, c.578G > A, c.778C > T, c.436C > T, c.1340G > C, c.436C > G, c.595C > G) were identified in these ten patients. Four missense variants (c.778C > T, c.1340G > C, c.436C > G and c.595C > G) were detected as new variant, in which these variants were not found previously in HGMD and 1000 Genome Project. The remaining four missense variants (c.638G > A; c.556C > T, c.578G > A and c.436C > G) were previously reported in literature.

The presence of all missense variants was confirmed in parental DNA. Only parent samples from Patients 4, 5, 7, 8 and 10 were available to test for inheritance cases (Table 1). All parents carried the variant in heterozygous form. In order to define pathogenicity of new missense variants; p.(Leu260Phe), p.(Ser447Thr), p.(Arg146Gly) and p.(Leu199Val), each of the variants was compared with 50 healthy normal individuals and also with gnomAD database. None of them were discovered in the healthy individuals as well as in gnomAD database.

3.3. In silico prediction

To further investigate the effects of four new ASL missense variants, multiple sequence alignment (protein) was performed using HomoloGene program to define the cross-species conservation of each new variant. Table 2 shows all four new missense variants were highly conserved among the species (90% to 100%).

In silico prediction servers were then performed to predict the pathogenicity of each of the new missense variants. All four *in silico* servers (FATHMM-X, Mutation taster 2, M-CAP and PROTEAN) predicted that all new missense variants as disease-causing (Table 2). The effect of new missense variants on the change in protein stability was examined with I-Mutant 3.0, CUPSAT and SDM. All servers predicted the three new variants; p.(Leu260Phe), p(Arg146Gly) and p.(Leu199Val) destabilized the ASL structure. However, only two servers (I-Mutant 3.0 and SDM) predicted p.(Ser447Thr) to destabilize the ASL structure.

3.4. Structural analysis

3.4.1. Quality of ASL native and mutant models

The effects of variants on the ASL structure were then further analyzed. The ASL native structure was developed from the known structures of ASL (PDB ID: 1K62 and 1AOS) using the program SWISS-MODEL. The mutant models were developed using the Swiss-PDB viewer. Energy minimization was then performed to the ASL native and mutant models. The quality of ASL native and mutant models was verified with PROCHECK. The Ramachandran plot determined by PROCHECK revealed the residues of the ASL native and mutant models in the most favorable regions were > 90%, as shown in Table 3. None of residues was detected in disallowed regions of the Ramachandran plot of the native and mutant models (Supplementary Fig. S1A). Scores produced by the PROCHECK were closed to the 100%, which showed the stereo-chemical quality of the ASL native and mutant models was in a good quality.

ProSA-web and ERRAT programs were also used to further check the quality of the ASL native and mutant models. The z-score generated from ProSA-web exhibited the overall model quality of the ASL native and mutant models was negative, as shown in Table 3 and Supplementary Fig. S1B. For the ASL native model, the value was within the range of z-score found for protein of similar groups, indicating the quality of this model was high. Meanwhile, for the mutant models, the values were within the range of the score of the native protein, suggested that all mutant models were in very good overall configuration. The ERRAT program exhibited the overall quality score for non-bonded atomic interactions of ASL native and mutant models was > 90%, as shown in Table 3. None of the residues were above the 99% cut off of error-value (Supplementary Fig. S1C). The ERRAT score exhibited the whole quality factor for the native and mutant models was greater than accepted range (50%), which indicated all of them were within the range of a high-quality model.

The RMSD calculation was also carried out to verify the quality of ASL native and mutant models. The superimposition of the native model onto the template structure (PDB ID: 1K62) produced RMSD of 0.05 Å. Meanwhile, for the mutant model, Table 3 shows RMSD values of the mutant models when superimposed onto the ASL native model.

3.4.2. Position of mutations and hydrogen bond interactions

Fig. 1 shows position of the reported and new variants in the ASL tetramer structure. The missense variants were mapped only to subunit A of tetramer ASL structure. All reported; p.(Arg213Gln), p.(Arg186Trp), p.(Arg193Gln) and p.(Arg146Trp) and three new; p.(Leu260Phe), p.(Arg146Gly) and p.(Leu199Val) variants were located

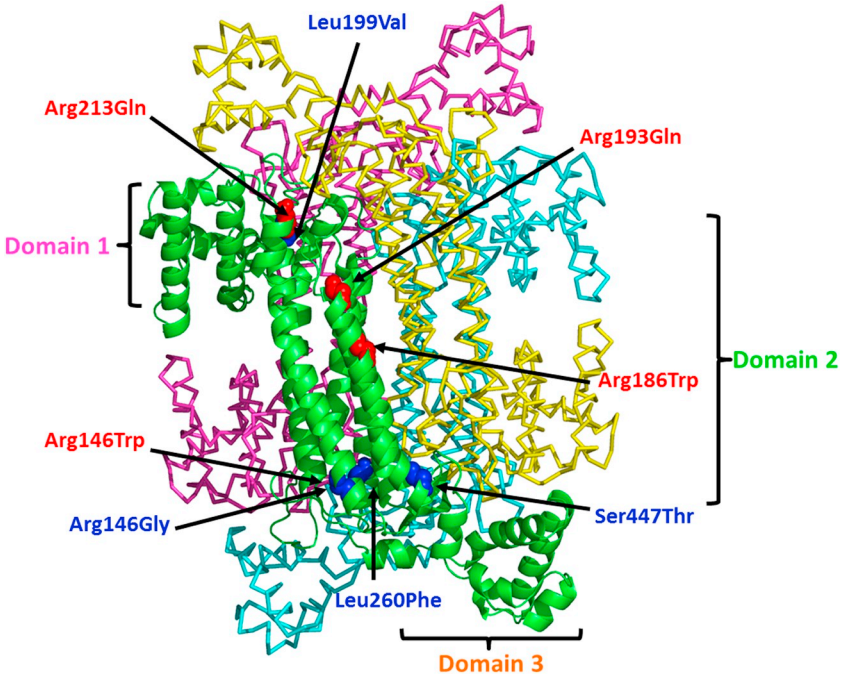

Fig. 1. The tetramer model of native ASL structure and positions of new and reported missense mutations recognized in this study. New and reported missense mutations are mapped to subunit A. New missense mutations are presented in blue sphere and labelled in blue font. The reported missense mutations are presented in red sphere and labelled in red font. The tetramer structure is shown in cartoon and ribbon. The subunit A is presented in green cartoon, while the subunit B, C and D are presented in cyan, magenta and yellow ribbons, respectively. The tetramer model is developed by Swiss-Model program [27] and visualized with PyMol [29]. (For interpretation of the references to colour in this figure legend, the reader is referred to the web version of this article.)

at domain 2, while only one variant; p.(Ser447Thr) was located at domain 3.

Table 4 shows all the hydrogen bond interactions between the native and neighboring residues, and between the mutated and neighboring residues. Information in this table includes the hydrogen bond interactions of the reported and new variants. Fig. 2a shows the substitution of arginine to glutamine affected the bonding patterns with the surrounding residues. Arginine (Arg213) in native structure was found to form hydrogen bond interactions with neighboring residues in subunit A, Leu199, Thr226, Arg217, Pro198 and Leu197. This residue was also found to form hydrogen bond interaction with neighboring residue Leu440 in subunit D. However, loss of hydrogen bond interactions with residues Thr226, Pro198 and Leu197 in subunit A, and residue L440 in subunit D was observed when arginine substituted to glycine at position 213.

Loss of hydrogen bond interactions with residue Asp183 in subunit A, and residues Glu241 and Asp237 in subunit D was also observed when the arginine substituted to tryptophan at position 186, as shown in Fig. 2b. The substituted Trp186 was found to form hydrogen bond interactions with residues Arg182, Val190 and Glu189 in subunit A. These residues (Arg182, Val190 and Glu189) were also found to form hydrogen bond interactions with Arg186 in the native structure. Residue Arg193 in native structure formed hydrogen bond interactions with residues Arg122, Glu189, Val190 and Glu241 in subunit A (Fig. 2c). Concurrently, this residue also formed interactions with residues in subunit D (Glu185 and Glu189). However, substitution to glutamine caused loss of interactions with all residues in subunit D, as shown in Fig. 2c. For mutation occurred at position 260, which changed from leucine to phenylalanine, the mutated residue (Phe260) was observed not to affect the bonding pattern with surrounding residues, as shown in Fig. 2d.

Fig. 2e shows arginine at position 146 in the native structure formed interactions with residues in subunit A, Thr142, Glu150, Ile350, Leu353 and Ala149. Nevertheless, the substituted tryptophan at this position affected the interactions with Glu150, Ile350 and Leu353. Meanwhile, the replacement of serine to threonine at position 447 caused loss of interactions with residue Gly441 (Fig. 2f). Instead, the mutated residue Thr447 formed new interaction with residue Ala439. The substituted glycine at position 146 (Gly146) was found to form similar bonding pattern, as presented in Trp146 mutant (Fig. 2g). For mutation occurred at position 199, which changed from leucine to valine, the mutated residue (Val199) was observed not to affect the bonding patterns with the surrounding residues, as shown in Fig. 2h.

4. Discussion

This study presented the first molecular analysis of ASLD in Malaysia population. Ten patients were identified to carry a missense variant in *ASL* gene with different clinical and biochemical phenotype, indicating the heterogeneous distribution of pathogenic variants in *ASL* gene. Although the splice site, deletion and insertion (indel) were not found in this study, the potential of cryptic splice sites and RNA decay also contributed for the severity of ASLD, as reported in other studies [34–36]. Currently, about 167 variants have been discovered in the HGMD, with the largest proportion are missense variants [10]. None of the reported and new missense variants obtained in this study were discovered at the active site of ASL protein. The new missense variants (Leu260Phe, Ser447Thr, Arg146Gly and Leu199Val) were detected as very rare variants as all of them were not discovered in our normal control, gnomAD, HGMD and 1000 Genome Project databases. Two new missense variants found in this study and located at positions 146 and 447 were basically a substitution of another amino acid at the exact site. The missense variants reported at these positions were found to be pathogenic [34].

In this study, four unrelated patients (Patients 1, 2, 3 and 4) shared a similar genotype, a Leu213Gln. This pathogenic variant was previously reported in patient associated with severe neonatal onset form in United State (US) population [34]. However, there is no detailed information on the functional study for this pathogenic variant. Our analysis showed although one *in silico* server (I-Mutant 3.0) predicted the Gln213 mutant increased the stability of the ASL structure, however, the other two *in silico* servers predicted to affect the stability of the ASL structure. Analysis of hydrogen binding patterns further supported the mutated residue (Gln213) caused loss of four hydrogen bond interactions in the ASL structure, including hydrogen bond interactions with the adjacent subunit. This would suggest that this pathogenic variant is predicted to highly likely affect the stability of the ASL structure. Furthermore, this pathogenic variant occurs in highly conserved region, implying the pathogenicity of this variant. The Arg213Gln mutant is suggested to have loss of protein function as three

Table 4
Hydrogen bond interactions between native and neighboring residues and between mutant and neighboring residues.

Patient	Exon	Mutation		Hydrogen bond interactions	
		Coding DNA number	Protein number	Hydrogen bond interactions between native and neighboring residue	Hydrogen bond interactions between mutant and neighboring residue
				Residue-chain-Atom	Residue-chain-Atom
P1	Ex-8	c.638G > A	p.(Arg213Gln)	R213-A-NE: L199-A-O	Q213-A-NE2: L199-A-O
P2				R213-A-NH1: T226-A-O	R217-A-N: Q213-A-O
P3				R213-A-NH1: L440-D-O	
P4				R213-A-NH2: L199-A-O	
				R217-A-N: R213-A-O	
				R213-A-NH2: P198-A-O	
				R213-A-NH2: L197-A-O	
P5	Ex-7	c.556C > T	p.(Arg186Trp)	R186-A-N: R182-A-O	W186-A-N: R182-A-O
P6				R186-A-NE: D183-A-OD2	V190-A-N: W186-A-O
				R186-A-NH1: E241-D-OE2	E189-A-N: W186-A-O
				R186-A-NH2: D183-A-OD1	
				R186-A-NH2: D237-D-OD1	
				V190-A-N: R186-A-O	
				Q189-A-N: R186-A-O	
P7	Ex-7	c.578G > A	p.(Arg193Gln)	R122-A-NH1: R193-A-O	R122-A-NH1: Q193-A-O
				R122-A-NH2: R193-A-O	R122-A-NH2: Q193-A-O
				R193-A-N: E189-A-O	Q193-A-N: E189-A-O
				R193-A-N: V190-A-O	Q193-A-N: V190-A-O
				R193-A-NE: E241-A-OE1	Q193-A-NE: E241-A-OE2
				R193-A-NE: E241-A-OE2	
				R193-A-NH2: E241-A-OE2	
				R193-A-NH1: E185-D-OE1	
				R193-A-NH1: E189-D-OE2	
				R193-A-NH2: E189-D-OE1	
	Ex-10	c.778C > T	p.(Leu260Phe)	L260-A-N: M256-A-O	F260-A-N: M256-A-O
				C264-A-N: L260-A-O	C264-A-N: F260-A-O
				L260-A-N: A257-A-O	F260-A-N: A257-A-O
P8	Ex-5	c.436C > T	p.(Arg146Trp)	R146-A-N: T142-A-O	W146-A-N: T142-A-O
				R146-A-NE: E150-A-OE1	E150-A-N: W146-A-O
				R146-A-NH1: I350-A-O	A149-A-N: W146-A-O
				R146-A-NH1: L353-A-O	
				R146-A-NH2: L353-A-O	
				R146-A-NH2: E150-A-OE1	
				R146-A-NH2: E150-A-OE2	
				E150-A-N: R146-A-O	
				A149-A-N: R146-A-O	
	Ex-15	c.1340G > C	p.(Ser447Thr)	G441-A-N: S447-A-OG	T447-A-N: A444-A-O
				Q451-A-N: S447-A-O	T447-A-N: S446-A-OG
				S447-A-N: A444-A-O	T447-A-OG1: A439-A-O
				S447-A-N: S446-A-OG	Q451-A-N: T447-A-O
P9	Ex-5	c.436C > G	p.(Arg146Gly)	R146-A-N: T142-A-O	G146-A-N: T142-A-O
				R146-A-NE: E150-A-OE1	E150-A-N: G146-A-O
				R146-A-NH1: I350-A-O	A149-A-N: G146-A-O
				R146-A-NH1: L353-A-O	
				R146-A-NH2: L353-A-O	
				R146-A-NH2: E150-A-OE2	
				R146-A-NH2: E150-A-OE2	
				E150-A-N: R146-A-O	
				A149-A-N: R146-A-O	
P10	Ex-7	c.556C > T	p.(Arg186Trp)	R186-A-N: R182-A-O	W186-A-N: R182-A-O
				R186-A-NE: D183-A-OD2	V190-A-N: W186-A-O
				R186-A-NH1: E241-D-OE2	E189-A-N: W186-A-O
				R186-A-NH2: D183-A-OD1	
				R186-A-NH2: D237-D-OD1	
				V190-A-N: R186-A-O	
				E189-A-N: R186-A-O	
	Ex-7	c.595C > G	p.(Leu199Val)	L199-A-N: T119-A-OG1	V199-A-N: T119-A-OG1
				R213-A-NE: L199-A-O	R213-A-NE: V199-A-O
				R213-A-NH2: L199-A-O	R213-A-NH2: V199-A-O

of our patients presented in severe neonatal disease phenotype. The same position was also affected with pathogenic variant, Arg213*, which was reported in patient associated with severe neonatal onset form in Italian population [37] and unknown phenotype in Indian and US populations [34].

Although Patient 4 had only 1 variant detected, nevertheless, metabolic/biochemical testing had established the diagnosis of ASLD. Therefore, the second disease-causing variant that could not be identified in this study might be due to undetectable by sequence analysis such as intragenic deletions or duplications. Hence, incorporating methods such as multiplex ligation-dependent probe amplification (MLPA), a gene-targeted microarray, quantitative PCR or long-range PCR could improve diagnostic yield.

Mutation of Arg186Trp was found as homozygous form in two

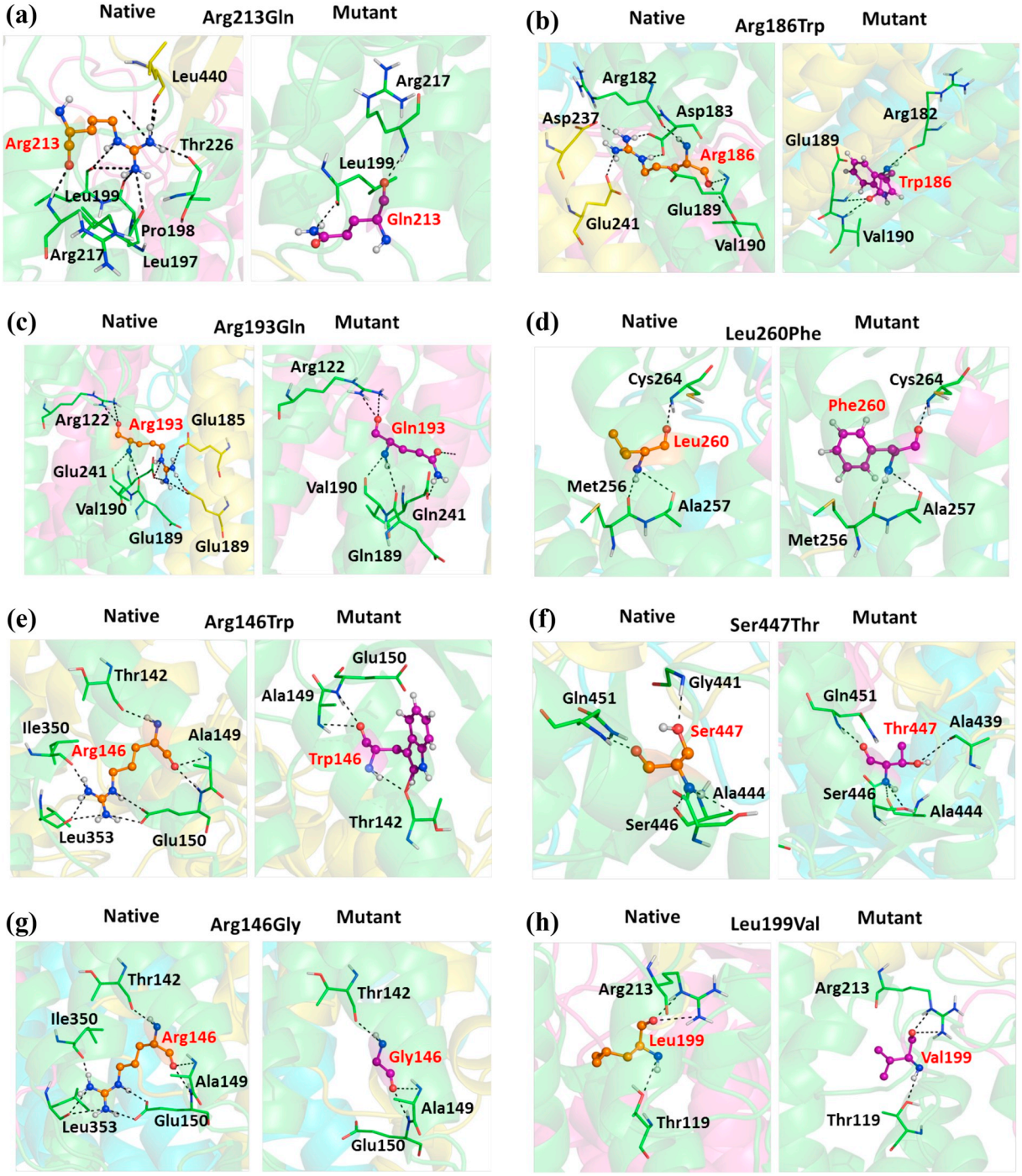

Fig. 2. Hydrogen bond interactions of native and mutants with neighboring residues. Native residue is presented in orange stick and sphere, while mutant residue is presented in purple stick and sphere. Hydrogen bonds are indicated by black dotted lines. Subunits A, B, C and D are presented in green, cyan, magenta and yellow cartoons, respectively. (For interpretation of the references to colour in this figure legend, the reader is referred to the web version of this article.)

unrelated patients (Patients 5 and 6). Both patients showed severe clinical and biochemical phenotype, which were presented with acute neonatal symptom. Therefore, our finding is similar with the previous reported case, in which changes to this arginine at this position are predicted to be deleterious and may affect the stability of the tetramer ASL structure [34,38]. This pathogenic variant was commonly reported in the Saudi Arabia [38] and Turkish populations [34].

Patient 7 had late-onset disease. This patient had compound heterozygous for new (Leu260Phe) and reported (Arg193Gln) pathogenic variants. This new pathogenic variant (Leu260Phe) was observed to not affecting the surrounding hydrogen bond interactions. However, this new pathogenic variant was discovered as disease-causing by *in silico* servers. In addition, this pathogenic variant occurs in highly conserved region, strengthening the pathogenicity of this variant. Meanwhile, the Arg193Gln was previously reported in patient associated with neonatal onset form in US and Austrian populations, and patient with the late onset form in Italian population [34,39]. However, there is no functional study for this variant [34]. Our structural analysis discovered this reported pathogenic variant affected the hydrogen bond interactions with the adjacent subunit, which indirectly disturbing the formation of tetrameric structure of ASL. Therefore, this would suggest that this pathogenic variant might contribute to the severity of this deficiency in

patient. The same position was also affected with pathogenic variant, Arg193Trp, which was found in US and German populations [34].

Patient 8 was also associated with severe neonatal onset form of disease. This patient had a compound heterozygous for new (Ser447Thr) and reported (Arg146Trp) pathogenic variants. The reported pathogenic variant, Arg146Trp was previously reported in US and Turkish populations in the literature [34]. However, there is no information stated about the functional study for this variant. In our structural analysis, both pathogenic variants (Ser447Thr and Arg146Trp) affected the ASL structure by altering the bonding patterns with the neighboring residues. In addition, *in silico* servers predicted both pathogenic variants as disease-causing. Consistent with this, both pathogenic variants were suggested to cause loss of protein function and resulted in a severe form in our patient.

A new variant in homozygous state (Arg146Gly) was observed in Patient 9, which had hyperammonemia episodes at day 7. This new pathogenic variant was predicted as disease-causing by *in silico* servers. Furthermore, the substitution of long side chain of arginine to small glycine has disturbed the bonding pattern of ASL structure. This indicates the impact of this new pathogenic variant to the stability of the ASL structure, which possibly causing the ASLD. The same position was also affected with pathogenic variant (Arg146Trp), which was reported in our study, US and Turkish populations [34]. Another pathogenic variant (Arg146Gln) located at the same position was previously reported in homozygous and heterozygous states in UK population [35].

Another new variant, Leu199Val was observed not to affect the surrounding hydrogen bond interactions of ASL structure in Patient 10. However, this pathogenic variant was found as compound heterozygous which formed along with the reported pathogenic variant, Arg186Trp. As mentioned above, the reported pathogenic variant, Arg186Trp was discovered as recurrent pathogenic variant disturbing the stability of the tetramer ASL structure [34,38]. This indicates that this reported pathogenic variant might participate to the severity of disease in this patient. Furthermore, *in silico* analysis exhibited the new pathogenic variant, Leu199Val as disease-causing. The impacts of both pathogenic variants were in line with the clinical phenotype of this patient, in which Patient 10 had a late-onset disease.

5. Conclusion

In conclusion, this study has characterized the clinical and molecular aspects of argininosuccinate aciduria in Malaysia patients. Eight different missense variants from 10 patients were identified. All the new and reported pathogenic variants discovered in this study may potentially disturb the ASL structure. This study has expanded the mutation spectrum of ASL mutations. Establishing a precise molecular diagnosis is beneficial not only for accurate genetic counselling but also for accurate carrier testing as early intervention is important to minimize disease progression.

Declaration of Competing Interest

All the authors declared that they have no conflicts of interest to this work.

Acknowledgment

We thank the Director General of Health, Malaysia for the permission to publish this paper. Our special thanks to Director of IMR, Head Center of Nutrition, Metabolism and Cardiovascular Research and Head Unit of Inborn Error of Metabolism and Genetics for careful reading of this manuscript. We would like to extend our gratitude to Mohd Khairul Nizam Mohd Khalid and Nurul Farahana Rosli for excellent technical assistance. We are also grateful to all clinicians for their contributions in this study. This study was funded by Diagnostics Services, Institute for Medical Research, Ministry of Health, Malaysia.

Appendix A. Supplementary data

Supplementary data to this article can be found online at https://doi.org/10.1016/j.ymgmr.2019.100525.

References

[1] W.E. O'Brien, R.H. Barr, Argininosuccinate lyase: purification and characterization from human liver, Biochemistry 20 (1981) 2056–2060, https://doi.org/10.1021/bi00510a049.
[2] W.E. O'Brien, R. Mcinnes, K. Kalumuck, M. Adcock, Cloning and sequence analysis of cDNA for human argininosuccinate Iyase (urea cycle/genetic disorders/chrpmosome mapping), Proc. Natl. Acad. Sci. U. S. A. 83 (1986) 7211–7215.
[3] M.L. Summar, S. Koelker, D. Freedenberg, C. Le Mons, J. Haberle, H.S. Lee, B. Kirmse, The incidence of urea cycle disorders, Mol. Genet. Metab. 110 (2013) 179–180, https://doi.org/10.1016/j.ymgme.2013.07.008.
[4] J. Häberle, N. Boddaert, A. Burlina, A. Chakrapani, M. Dixon, M. Huemer, D. Karall, D. Martinelli, P.S. Crespo, R. Santer, A. Servais, V. Valayannopoulos, M. Lindner, V. Rubio, C. Dionisi-Vici, Suggested guidelines for the diagnosis and management of urea cycle disorders, Orphanet. J. Rare Dis. 7 (2012) 1–30, https://doi.org/10.1186/1750-1172-7-32.
[5] S.L. Naylor, R.J. Klebe, T.B. Showsf, Argininosuccinic aciduria: assignment of the argininosuccinate lyase gene to the pter-q22 region of human chromosome 7 by bioautography (somatic cell hybrids/aminoaciduria), Proc. Natl. Acad. Sci. U. S. A. 75 (1978) 6159–6162.
[6] L. Simard, W.E. O'brien, R.R. Mcinnes, Argininosuccinate lyase deficiency: evidence for heterogeneous structural gene mutations by immunoblotting, Am. J. Hum. Genet. 39 (1986) 38–51.
[7] S. Ratner, B. Petrack, The mechanism of arginine synthesis from citrulline in kidney, J. Biol. Chem. 200 (1953) 175–185.
[8] G. Wu, D.A. Knabe, N.E. Flynn, Synthesis of citrulline from glutamine in pig enterocytes, Biochem. J. 299 (1994) 115–121.
[9] E. Bizzoco, M. Simonetta Faussone-Pellegrini, M. Giuliana Vannucchi, Activated microglia cells express argininosuccinate synthetase and argininosuccinate lyase in the rat brain after transient ischemia, Exp. Neurol. 208 (2007) 100–109, https://doi.org/10.1016/j.expneurol.2007.07.018.
[10] P.D. Stenson, M. Mort, E.V. Ball, K. Evans, M. Hayden, S. Heywood, et al., The human gene mutation database: towards a comprehensive repository of inherited mutation data for medical research, genetic diagnosis and next-generation sequencing studies, Hum. Genet. 136 (2017) 665–677, https://doi.org/10.1007/s00439-017-1779-6.
[11] T.I. Perry, M.I. Wirtz, N.G. Kennaway, Y.E. Hsia, F.C. Atienza, H.S. Uemura, Amino acid and enzyme studies of brain and other tissues in an infant with argininosuccinic aciduria, Clin. Chim. Acta 105 (1980) 257–267.
[12] S. Renouf, A. Fairand, A. Husson, Developmental control of argininosuccinate lyase gene by methylation, Biol. Neonate 73 (1998) 190–197.
[13] M. Linnebank, A. Homberger, B. Rapp, C. Winter, T. Marquardt, E. Harms, H.G. Koch, Two novel mutations (E86A, R113W) in argininosuccinate lyase deficiency and evidence for highly variable splicing of the human argininosuccinate lyase gene, J. Inherit. Metab. Dis. 23 (2000) 308–312.
[14] R.H. Don, P.T. Cox, B.J. Wainwright, K. Baker, J.S. Mattick, "Touchdown" PCR to circumvent spurious priming during gene amplification, Nucleic Acids Res. 19 (1991) 4008.
[15] The 1000 Genomes Project Consortium, A global reference for human genetic variation, Nature 526 (2015) 68–74, https://doi.org/10.1038/nature15393.
[16] M. Lek, K.J. Karczewski, E.V. Minikel, K.E. Samocha, E. Banks, T. Fennell, H.O. anne, J. Ware, andrew J. Hill, B.B. Cummings, T. Tukiainen, D.P. Birnbaum, J. Kosmicki, L.E. Duncan, K. Estrada, F. Zhao, J. Zou, E. Pierce-Hoffman, J. Berghout, et al., Analysis of protein-coding genetic variation in 60,706 humans, Nature 536 (2016) 285–291, https://doi.org/10.1038/nature19057.
[17] M.F. Rogers, H.A. Shihab, M. Mort, D.N. Cooper, T.R. Gaunt, C. Campbell, FATHMM-XF: accurate prediction of pathogenic point mutations via extended features, Bioinformatics 34 (2018) 511–513, https://doi.org/10.1093/bioinformatics/btx536.
[18] J.M. Schwarz, D.N. Cooper, M. Schuelke, D. Seelow, MutationTaster2: mutation prediction for the deep-sequencing age, Nat. Methods 11 (2014) 361–362, https://doi.org/10.1038/nmeth.2890.
[19] K.A. Jagadeesh, A.M. Wenger, M.J. Berger, H. Guturu, P.D. Stenson, D.N. Cooper, J.A. Bernstein, G. Bejerano, M-CAP eliminates a majority of variants of uncertain significance in clinical exomes at high sensitivity, Nat. Genet. 48 (2016) 1581–1586, https://doi.org/10.1038/ng.3703.
[20] Y. Choi, A.P. Chan, PROVEAN web server: a tool to predict the functional effect of amino acid substitutions and indels, Bioinformatics 31 (2015) 2745–2747, https://doi.org/10.1093/bioinformatics/btv195.
[21] E. Capriotti, P. Fariselli, I. Rossi, R. Casadio, A three-state prediction of single point mutations on protein stability changes, BMC Bioinformatics 9 (Suppl. 2) (2008) 1–9, https://doi.org/10.1186/1471-2105-9-S2-S6.
[22] V. Parthiban, M.M. Gromiha, D. Schomburg, CUPSAT: prediction of protein stability upon point mutations, Nucleic Acids Res. 34 (2006) W239–W242, https://doi.org/10.1093/nar/gkl190.
[23] C.L. Worth, R. Preissner, T.L. Blundell, SDM-a server for predicting effects of mutations on protein stability and malfunction, Nucleic Acids Res. 39 (2011) W215–W222, https://doi.org/10.1093/nar/gkr363.
[24] P.W. Rose, A. Prlí, C. Bi, W.F. Bluhm, C.H. Christie, S. Dutta, R. Kramer Green,

D.S. Goodsell, J.D. Westbrook, J. Woo, J. Young, C. Zardecki, H.M. Berman, P.E. Bourne, S.K. Burley, The RCSB protein data Bank: views of structural biology for basic and applied research and education, Nucleic Acids Res. 43 (2015) D345–D356, https://doi.org/10.1093/nar/gku1214.

[25] L.M. Sampaleanu, P.W. Codding, Y.D. Lobsanov, M. Tsai, G.D. Smith, C. Horvatin, P.L. Howell, Structural studies of duck delta2 crystallin mutants provide insight into the role of Thr161 and the 280s loop in catalysis, Biochem. J. 384 (2004) 437–447, https://doi.org/10.1042/BJ20040656.

[26] M.A. Turner, A. Simpson, R.R. Mcinnes, P.L. Howell, Human argininosuccinate lyase: a structural basis for intragenic complementation, Proc. Natl. Acad. Sci. U. S. A. 94 (1997) 9063–9068.

[27] A. Waterhouse, M. Bertoni, S. Bienert, G. Studer, G. Tauriello, R. Gumienny, F.T. Heer, T.A.P. De Beer, C. Rempfer, L. Bordoli, R. Lepore, T. Schwede, SWISS-MODEL: homology modelling of protein structures and complexes, Nucleic Acids Res. 46 (2018) W296–W303, https://doi.org/10.1093/nar/gky427.

[28] M.U. Johansson, V. Zoete, O. Michielin, N. Guex, Defining and searching for structural motifs using DeepView/Swiss-PdbViewer, BMC Bioinformatics 13 (2012) 173.

[29] W.L. DeLano, The PyMOL Molecular Graphics System, DeLano Sci, San Carlos, 2002.

[30] R.A. Laskowski, M.W. MacArthur, J.M. Thornton, PROCHECK : Validation of Protein-structure Coordinates, (2012), pp. 684–687, https://doi.org/10.1107/97809553602060000882.

[31] M. Wiederstein, M.J. Sippl, ProSA-web: interactive web service for the recognition of errors in three-dimensional structures of proteins, Nucleic Acids Res. 35 (2007) W407–W410, https://doi.org/10.1093/nar/gkm290.

[32] C. Colovos, T. 0 Yeates, Verification of protein structures: patterns of nonbonded atomic interactions, Protein Sci. 2 (1993) 1511–1519.

[33] E.F. Pettersen, T.D. Goddard, C.C. Huang, G.S. Couch, D.M. Greenblatt, E.C. Meng, T.E. Ferrin, UCSF chimera - a visualization system for exploratory research and analysis, J. Comput. Chem. 25 (2004) 1605–1612, https://doi.org/10.1002/jcc.20084.

[34] C. Balmer, A.V. Pandey, V. Rüfenacht, J.M. Nuoffer, P. Fang, L.J. Wong, J. Häberle, Mutations and polymorphisms in the human argininosuccinate lyase (ASL) gene, Hum. Mutat. 35 (2014) 27–35, https://doi.org/10.1002/humu.22469.

[35] J. Baruteau, E. Jameson, A.A. Morris, A. Chakrapani, S. Santra, S. Vijay, H. Kocadag, C.E. Beesley, S. Grunewald, E. Murphy, M. Cleary, H. Mundy, L. Abulhoul, A. Broomfield, R. Lachmann, Y. Rahman, P.H. Robinson, L. Macpherson, K. Foster, W. Kling Chong, D.A. Ridout, K. Mckay Bounford, S.N. Waddington, P.B. Mills, P. Gissen, J.E. Davison, Expanding the phenotype in argininosuccinic aciduria: need for new therapies, J. Inherit. Metab. Dis. 40 (2017) 357–368, https://doi.org/10.1007/s10545-017-0022-x.

[36] P. Rostami, J. Häberle, A. Setoudeh, J. Zschocke, F. Sayarifard, Two novel mutations in the argininosuccinate lyase gene in Iranian patients and literature review, Iran. J. Pediatr. 27 (2017) 26–28, https://doi.org/10.5812/ijp.7666.

[37] E. Trevisson, A. Burlina, M. Doimo, V. Pertegato, A. Casarin, L. Cesaro, P. Navas, G. Basso, G. Sartori, L. Salviati, Functional complementation in yeast allows molecular characterization of missense argininosuccinate lyase mutations, J. Biol. Chem. 284 (2009) 28926–28934, https://doi.org/10.1074/jbc.M109.050195.

[38] F. Imtiaz, M. Al-Sayed, D. Trabzuni, B.R. Al-Mubarak, O. Alsmadi, M.S. Rashed, B.F. Meyer, Novel mutations underlying argininosuccinic aciduria in Saudi Arabia, BMC Res. Notes. 3 (2010) 1–5, https://doi.org/10.1186/1756-0500-3-79.

[39] P. Barbosa, M. Cialkowski, W.E. O'Brien, Analysis of naturally occurring and site-directed mutations in the argininosuccinate lyase gene, J. Biol. Chem. 266 (1991) 5286–5290.